ACS APPLIED MATERIALS & INTERFACES

www.acsami.org

Research Article

# Electrogenerated Chemiluminescence Biosensor Based on Functionalized Two-Dimensional Metal–Organic Frameworks for Bacterial Detection and Antimicrobial Susceptibility Assays

Lina Sun, Yu Chen, Yuhong Duan, and Fen Ma*

Cite This: *ACS Appl. Mater. Interfaces* 2021, 13, 38923–38930

Read Online

ACCESS | Metrics & More | Article Recommendations | Supporting Information

**ABSTRACT:** The emergence of antibiotic resistance has prompted the development of rapid antimicrobial susceptibility testing (AST) technologies to guide antibiotic prescription. A novel electrochemiluminescence (ECL) biosensor developed can quantitatively measure the binding between the lectin and lipopolysaccharide (LPS) on Gram-negative bacteria for bacterial determination and to characterize the antimicrobial activities of $\beta$-lactam and non-$\beta$-lactam antibiotics to normal and antibiotic-resistant bacteria. The biosensor utilizes ruthenium complex tagged concanavalin A (Ru-Con A) coated on $NH_2$-MIL-53(Al) interface for LPS binding measurements. The decreased ECL signal obtained was directly proportional to increasing *Escherichia coli* (*E. coli*) BL21 concentrations. The sensitivity displayed logarithmic dependence in the range of (50−5.0) × $10^4$ cells/mL, with a detection limit of 16 cells/mL. The minimum inhibitory concentration (MIC) values of antibiotics for normal *E. coli* BL21 were 0.02−0.2, 2−4, 0.002−0.02, and 0.2−1 mg/L for levofloxacin hydrochloride (LVX), tetracycline (TCY), imipenem (IPM), and cefpirome (CPO), respectively. The increased MIC values (8−16 and 4 mg/L for IMP and CPO, respectively) in New Delhi metallo-$\beta$-lactamase-1 expressing *E. coli* BL21 (NDM-1-*E. coli* BL21) indicated greater resistance to $\beta$-lactams in NDM-1-*E. coli* BL21 compared with normal *E. coli* BL21. Therefore, the changed ECL signal because of binding between LPS with the lectin has a relation with the type of antibiotic and bacterial strains, making the ECL biosensor promote clinical practicability and facilitate antibiotic stewardship.

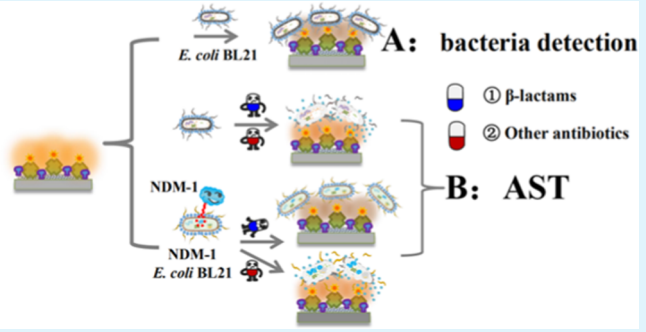


**KEYWORDS:** *electrogenerated chemiluminescence, antibiotic, antibiotic susceptibility, Escherichia coli, New Delhi metallo-β-lactamase-1, minimum inhibitory concentration*

Downloaded via TSINGHUA UNIV on November 4, 2022 at 17:43:39 (UTC).
See https://pubs.acs.org/sharingguidelines for options on how to legitimately share published articles.

## INTRODUCTION

Pathogenic bacteria can multiply rapidly and spread easily in the environment with the increase of environmental pollution, which is a cause of many health-related problems. Sensitive and rapid bacterial detection methods should be established for preliminary clinical diagnosis.[1,2] And then, it is critical to quickly initiate targeted antimicrobial therapy, which could reduce morbidity and mortality in patients.[3] However, more and more pathogenic bacteria are being reported to have developed resistance to one or multiple antibiotics (frequently called "super-bugs") because of increasing use and haphazard misuse of antibiotics.[4,5] Thus, antibiotic susceptibility testing (AST) of the infecting bacteria is recommended, such that suitable antibiotics could be prescribed after a careful evaluation of their efficacy.[6] Classical phenotypic growth-based ASTs proved by Clinical Laboratory and Standards Institute (CLSI) have been served as the gold standard, including the broth microdilution assay and disk diffusion assay or E-test.[7] These assays typically take multiple time-consuming steps including preculturing of clinical samples,[8] determination of growth using absorption spectroscopy,[9] and incubation of bacteria with antibiotics for AST.[10] Further, assays based on the turbidity of bacterial culture may lead to false positives since exposure to antibiotics easily alters the morphological characteristics of bacteria.[11] The rapid and sensitive genotypic ASTs, such as PCR,[12] padlock probe-dependent rolling circle amplification,[13] and loop-mediated isothermal amplification (LAMP),[14] also suffer some drawbacks, such as a limited number of genes associated with phenotypic resistance,[15] sophisticated sample preparation steps, and the requirement of expensive enzymes and primers,[16] and limit their effectiveness. In recent years, microfluidic techniques,[17] such as mass

Received: June 28, 2021
Accepted: July 28, 2021
Published: August 9, 2021

ACS Publications

© 2021 American Chemical Society

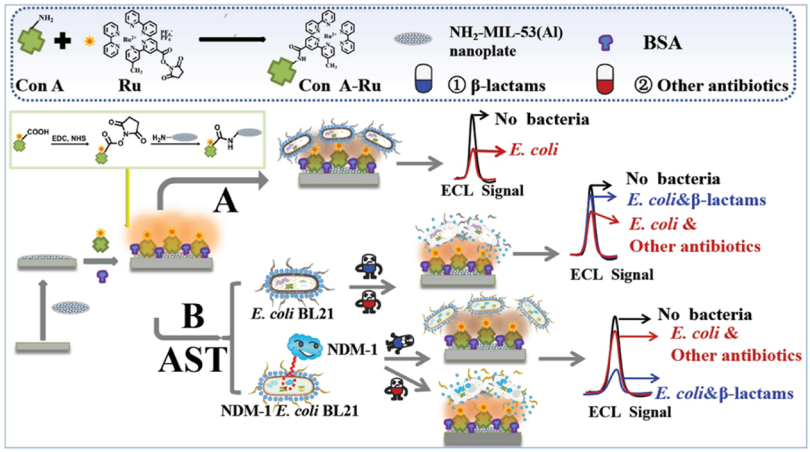


**Figure 1.** Schematic representation of the ECL biosensor for detection of *E. coli* BL21 (A) and antimicrobial susceptibility assays of representative antibiotics against *E. coli* BL21 and NDM-1 *E. coli* BL21 (B).

spectrometry (MS),[18] matrix-assisted laser desorption ionization time-of-flight (MALDI-TOF) MS,[3] Raman spectroscopy,[4] and light scattering microscopy,[19] have been adapted for ASTs. However, these novel methods suffer from certain disadvantages such as nonportable instrument, operational trouble, etc.[20]

Biosensor assays can be a smart option for susceptibility testing if a suitable strategy can be devised by understanding the antibiotic action mechanisms. Lipopolysaccharide (LPS) lying on the cell wall of Gram-negative bacteria consists of lipid A, core oligosaccharide, and O-antigen made of repetitive subunits of one to eight sugars.[1] Many bacteria are subclassified by the O-antigen on their surface. Therefore, LPS O-antigens are unique to specific bacterial strains (i.e., subspecies)[21] and exhibit highly specific binding affinity to lectins.[22] Much effort has been made to utilize lectins as recognition elements and glycoconjugates as receptors for the design of bacterial biosensors, such as quartz crystal microbalance (QCM)[23] and optical,[24] electrochemical,[25] and thermal[26] biosensors. Various in vitro studies have reported the release of significant amounts of LPS (endotoxin) when bacteria are exposed to bactericidal antibiotics.[27] The ability of antibiotics to induce the release of LPS from bacteria may be class- and concentration-dependent since different classes of antibiotics have different mechanisms of action and the effect of antibiotic concentrations on the bacterial morphology is distinct for each type of antibiotic. We have previously reported that detection of lectin−LPS interactions on the walls of *E. coli* cells can be used to evaluate the antimicrobial susceptibility of various antibiotics.[28] In this work, we will further systematically study the antibacterial sensitivity of various antibiotics to normal and drug-resistant bacteria.

Electrogenerated chemiluminescence (ECL) is a useful technique for biosensing because it has high sensitivity, selectivity, controllability, and simple operation.[29] One of the reported amplification strategies is based on the utilization of nanomaterials used as electrode-modified materials to mainly increase the detected ECL signals.[30] Metal−organic frameworks (MOFs), as a novel type of porous crystalline material, have attracted much attention due to their unique properties, such as their well-defined crystal structure, high volume of tunable micropores, large surface area, high agent loading, and versatile functionality. Ruthenium(II) ploypyridyl (Rubpy) complexes are of specific interest in the synthesis of various MOFs due to their excellent luminescent properties.[31] For example, Chi et al. synthesized Rubpy-functionalized MOFs (Ru-MOFs) and developed a fast ECL sensing method for $Hg^{2+}$ detection.[31] In this work, we focus on two novel aspects of the suitability of an ECL biosensor (as shown in Figure 1). The ECL biosensor was designed in which concanavalin A (Con A) served as a molecular recognition element, $NH_2$-MIL-53(Al) used as an electrode-modified material, and the ruthenium(II) complex (Ru) as an ECL-emitting species. The biosensor was fabricated on a glassy carbon electrode coated with a layer of $NH_2$-MIL-53(Al). The ECL probe (Ru tagged-Con A, abbreviated Ru-Con A) was covalently attached by the following steps: The carboxy terminus of Con A reacts with NHS and forms Con A-NHS ester. Subsequently, this Con A-NHS ester forms an amide bond with the amino group of $NH_2$-MIL-53(Al) in the presence of EDC, thereby Ru-Con A is covalently linked to the surface of $NH_2$-MIL-53(Al) (as shown in Figure 1). *E. coli* BL21 was used as the target model. The O-antigen subunit of *E. coli* BL21 contains *N*-acetylglucosamine and mannose, which have been shown to be specifically recognized by Con A. When *E. coli* BL21 binds to the ECL probe, LPS-Con A conjugate is formed. According to our hypothesis, if the antibiotics affect *E. coli*, subsequently the binding between the LPS of *E. coli* and the Con A confined to the sensor surface will be changed. The result is the number of bacteria bound to the ECL biosensor would change proportionally, thereby inducing differential changes in ECL signals. The susceptibility of the antibiotics against normal and drug-resistant bacteria could be evaluated based on the magnitude of change in ECL signals.

## EXPERIMENTAL SECTION

Details of the materials and apparatus used in the experiments, synthesis of the ECL probe (Ru-Con A), preparation of the $NH_2$-MIL-53(Al) nanoplate, fabrication of the ECL biosensor, and ECL-based bacterial detection and ASTs are presented in the Supporting Information. All microbial strains were cultivated following the manufacturer's guidelines and previous reports.

**ECL Measurements.** The fabricated ECL biosensor was immersed in 300 $\mu$L of a fixed concentration of *E. coli* BL21 for incubation of 60 min and then rinsed with binding buffer. The ECL measurement was performed in 3 mL of 10 mM Tris-HCl containing 1 mM $CaCl_2$, 1 mM $MnCl_2$ ($Ca^{2+}$ and $Mn^{2+}$ avoid possible deactivation of Con A), and 50 mM TPrA (as a coreactant) at 0 to +1.35 V. The concentration of *E. coli* BL21 was quantified by ECL


https://doi.org/10.1021/acsami.1c11949
ACS Appl. Mater. Interfaces 2021, 13, 38923−38930

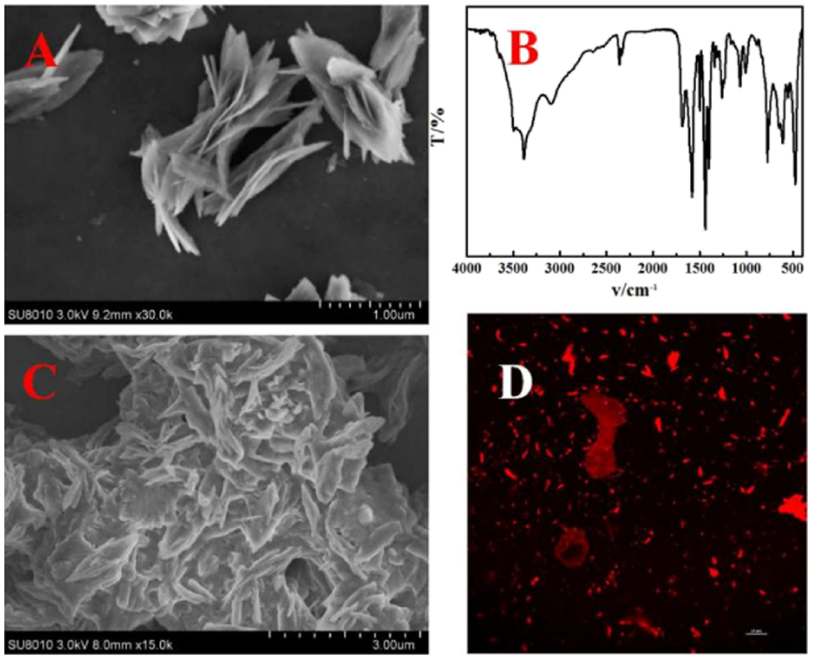


**Figure 2.** Structural images of $NH_2$-MIL-53(Al): (A) TEM image of $NH_2$-MIL-53(Al); (B, C) SEM images of $NH_2$-MIL-53(Al); and (D) FTIR of $NH_2$-MIL-53(Al).

intensity ($I$). The antimicrobial susceptibilities of antibiotics were assayed by immersing the ECL biosensor in 300 $\mu$L of *E. coli* BL21 or NDM-1 *E. coli* BL21 treated by different antibiotics for 60 min and then rinsing with binding buffer, and the corresponding ECL signal was measured. The minimum inhibitory concentrations (MICs) were measured upon 80% reduction than the negative control (without adding any antibiotic to the bacterial suspension) measured by the ECL biosensor.

## RESULTS AND DISCUSSION

**Characterization and Effectivity of the ECL Biosensor.** The structure and morphology of the synthesized $NH_2$-MIL-53(Al) nanoplate and Ru-Con A/$NH_2$-MIL-53(Al) were characterized by transmission electron microscopy (TEM, as shown in Figure S1), scanning electron microscopy (SEM), Fourier transform infrared spectroscopy (FTIR), and fluorescence imaging, as shown in Figure 2. From Figure 2A, it is revealed that plate-like thin layers within the nanosized scale were observed, suggesting the two-dimensional structure of $NH_2$-MIL-53(Al). From Figure 2B, it can be seen that two peaks at around 3510 and 3400 $cm^{-1}$ are assigned to the stretching modes of N−H bonding, which indicates the presence of free amine groups. The amine group is crucial for effective surface modification/immobilization of electroactive species. Besides, those around 1600−1330 $cm^{-1}$ reflect the symmetric and asymmetric vibrations of the carboxyl groups. A peak around 1250−1270 $cm^{-1}$ can be ascribed to the bidentate carbonate linker coordinated to the metal center. Figure 2C shows the SEM image of the Ru-Con A/$NH_2$-MIL-53(Al) nanoplate. Compared to Figure 2A, the two-dimensional structure becomes blurred. Figure 2D shows the fluorescence image of Ru-Con A/$NH_2$-MIL-53(Al). The emission, attributed to the Ru emission at 627 nm, indicates that Ru is coupled on the surface of the $NH_2$-MIL-53(Al) nanoplate. The insights obtained from SEM, FTIR, and fluorescence imaging indicated that $NH_2$-MIL-53(Al) and Ru-Con A/$NH_2$-MIL-53(Al) were synthesized successfully. Electrochemical impedance spectra (EIS) were acquired and utilized to characterize the ECL biosensor at different steps. The results showed that the charge transfer resistance ($R_{ct}$) increased from 40 Ω at a bare glassy carbon electrode (GC) to 1200 Ω at the $NH_2$-MIL-53(Al)-modified GC, followed by an unexpected decrease to 580 Ω in the presence of covalently linked Ru-Con A. The possible reasons are as follows: one is that $NH_2$-MIL-53(Al) fell off the GC surface during binding Ru-Con A. The other one is the electrostatic attraction between the Ru complex and the $[Fe(CN)_6]^{3-/4-}$ anion[32] and the redox reaction between the Ru complex and $[Fe(CN)_6]^{3-/4-}$. $R_{ct}$ was found to increase further to 1512 Ω on blocking with 0.5% BSA and finally to 2650 Ω when *E. coli* BL21 was bound to the ECL biosensor (Figure S2). The significant changes in the magnitude of $R_{ct}$ indicate that the biosensor was successfully fabricated and could respond to the presence of target *E. coli* BL21.[33]

Further, we examined the feasibility of the ECL biosensor for bacterial detection. Figure S3 shows the responses of the ECL biosensor to different concentrations of *E. coli* BL21. In the absence of binding to *E. coli* BL21, a much higher ECL intensity (2364, line a) was observed. The ECL signal decreased from 2364 (line a) to 1265 (line b) when the ECL biosensor was bound to *E. coli* BL21 at a concentration of 50 cells/mL. The ECL intensity continued to decrease to 903 (line c) as the concentration of *E. coli* BL21 increased from 50 $\times 10^2$ to 5 $\times 10^2$ cells/mL. According to the existing literature, approximately 170 types of O-antigens have been identified in *E. coli* and the O-antigen of the B strain is classified as type O7, as shown by ≥99% bp identity between the O-antigen gene cluster of B and the sequenced O7 gene cluster of *E. coli* VW187.[34] The O7 antigen subunit contains five sugars, namely, *N*-acetylglucosamine, galactose, mannose, 4-acetamido-4,6-dideoxy glucose, and rhamnose,[35] in which mannose and *N*-acetylglucosamine have been shown to be recognized by specific Con A.[36] Therefore, the decreased ECL intensity observed in this work resulted from *E. coli* BL21 specifically bound to the Con A-modified ECL biosensor, which could hinder the electron transfer of the Ru complex and diffusion of


https://doi.org/10.1021/acsami.1c11949
ACS Appl. Mater. Interfaces 2021, 13, 38923−38930

TPA to the electrode surface. When increasing concentrations of *E. coli* were introduced into the ECL biosensor chamber, a concomitant decrease in the ECL signal was observed, indicating that the ECL biosensor shows a signal OFF readout mechanism.

**Analytical Performance.** Once we adequately characterized the ECL biosensor and optimized the Ru-Con A concentration (7.0 $\mu$M) required for fabrication of the biosensor (Figure S4), it was necessary to evaluate the appropriate analytical (sensitivity) parameters for arriving at a quantitative estimation of performance outcomes. To this end, the dynamic sensitivity range of the ECL biosensor developed in this work toward *E. coli* BL21 was investigated (Figure 3). Figure 3 shows the ECL response of the ECL

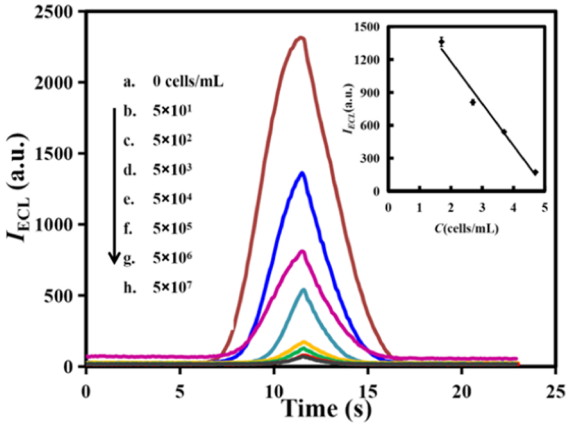


**Figure 3.** ECL profiles of the ECL biosensor after interacting with different concentrations of *E.coli* BL21. Inset: calibration curves of concentrations of *E. coli* BL21. Measurement solution: 10 mM Tris-HCl containing 1 mM $CaCl_2$, 1 mM $MnCl_2$, and 50 mM TPrA. Scan rate: 0.1 V/s.

biosensor after being loaded with different concentrations of *E. coli* BL21 from 0 to 5.0 × $10^7$ cells/mL. From Figure 3, we found that a much higher ECL intensity (2316) was gained without binding the ECL biosensor to *E. coli* BL21 (equivalent to the concentration of *E. coli*, i.e., 0 cells/mL). In the presence of *E. coli* BL21, the ECL signal decreased by increasing the concentration of *E. coli* BL21 to 5.0 × $10^5$ cells/mL (Figure 3), which excluded the quenching of the Ru complex by other compounds in the solution (Figure S5). Then, the platform presented by the curve indicated that *E. coli* BL21 reached saturation on the biosensor interface when the concentration of *E. coli* was over 5.0 × $10^6$ cells/mL, which was independent of surface density. However, accurate measures of the surface coverage of *E. coli* BL21 on the ECL biosensor interface were not available by the current technique. In view of the exponential growth trend of bacteria growing in different environments and meeting the needs of the actual evaluation system, in our work, the calibration curve was obtained based on the log 10-transformed *E. coli* BL21 counts and ECL signals of the ECL biosensor. The linear regression equation fitted to the observed data was given by $I = -383.8 \log C + 1949.7$ (unit of $C$ is cells/mL, $R^2 = 0.9793$) and the corresponding detection limit (DL) was 16 cells/mL ($3\sigma$)[37] except for the point corresponding to 0 cells/mL of *E. coli* BL21. A comparative analysis of existing biosensing methods for *E. coli* detection established that the ECL biosensor developed in this work showed excellent sensitivity. For example, the DL of the ECL biosensor is many folds lower than the value of 1000 cells/mL for *E. coli* O157:H7 required from a colorimetric and electrochemistry bioassay using *p*-benzoquinone as a redox mediator[38] and is even lower than the value of 40 cells/mL for *E. coli* O157:H7 from a fluorescence-based method employing CRISPR-Cas9-triggered two-step isothermal amplification.[39] The high sensitivity of the ECL biosensor could be attributed to the rigid LPS-mediated Con A−*E. coli* binding, which has been discussed in detail in our previous work,[23] where two binding activities on the *E. coli* cell wall were discussed.[40] We have previously reported a quinone-fused polythiophene interface for the detection of *E. coli* W1485 by electrochemical and QCM transducers, with DLs of 25 cells/mL (using the SWV technique) for *E. coli* W1485 and 50 cells/mL (using QCM) via Con A-mediated LPS−mannose binding.[23] The DL reported in this work is still lower than that of the previous work, although the LPS and Con A recognition systems are used in both works, which is possibly due to the advantages of the ECL technique and $NH_2$-MIL-53(Al) used in this work.

Figure S6 shows the ECL intensity recorded from the ECL biosensor after incubation with *E. coli* BL21 (5 × $10^3$ cells/mL) for 15 cycles. A relative standard deviation of 2.8% in ECL intensity indicated that Ru-Con A attached to the $NH_2$-MIL-53(Al) interface by C−N covalent coupling provided sufficient stability for the fabrication of ECL biosensors. To evaluate the selectivity of this sensor, five types of bacteria, namely, *E. coli* BL21, *Enterococcus faecalis*, *Streptococcus mutans*, *Staphylococcus aureus*, and *Salmonella pullorum*, were tested. There was no significant change in the ECL intensity of these bacteria, while that of *E. coli* BL21 changed significantly. The possible reason may be that LPS is the major component of the outer membrane for Gram-negative bacteria but not for Gram-positive bacteria. Unfortunately, the ECL biosensor in this work could not respond to *Salmonella pullorum*, possibly because LPS O-antigens are unique to specific bacterial strains. The storage stability of the ECL biosensors fabricated was also checked (Figure S6). After being stored in a refrigerator at 4 °C for 7 and 14 days, the biosensor showed recoveries of 97.3 and 95.9% in the ECL intensity of the initial ECL biosensor. This indicates that the ECL biosensor also has good storage stability.

**Applicability of the ECL Biosensor for Determination of the Antimicrobial Susceptibility of Antibiotics.** Different types of antibiotics have different mechanisms, and the effects of antibiotics on the morphology and vitality of bacteria are also different.[41] The interaction between antibiotics and bacteria leads to changes in the outer membrane of the bacterial cell wall, the magnitude of which depends on the specific antibiotic used.[41] These effects, including chemical modifications of the LPS chain, could significantly affect bacterial interaction with the substrates.[42] Our previous work provided a preliminary demonstration of the suitability of biosensors as indirect reporters of antibiotic susceptibility under various physiological conditions, based on the measurements of binding affinity between LPS from Gram-negative bacteria and lectins.[28] In the present work, the antibiotic susceptibility of $\beta$-lactam (cefpirome (CPO) and imipenem (IPM)) and non-$\beta$-lactam (tetracycline (TCY) and levofloxacin hydrochloride (LVX)) antibiotics against normal and drug-resistant bacterial strains was evaluated via the effects of antibiotics on *E. coli* cell wall LPS. To verify whether the developed ECL biosensor could be used for the evaluation of antimicrobial susceptibility, fresh *E. coli* samples were prepared


https://doi.org/10.1021/acsami.1c11949
ACS Appl. Mater. Interfaces 2021, 13, 38923−38930

and incubated with different kinds of antibiotics in a shaking incubator. The *E. coli* sample prepared without antibiotics was used as a control. Figure 4 shows the ECL response of the ECL biosensor incubated with *E. coli* BL21 (red columns) and NDM-1 *E. coli* BL21 (blue columns) pretreated with 2 mg/L TCY, LVX, CPO, and IMP.

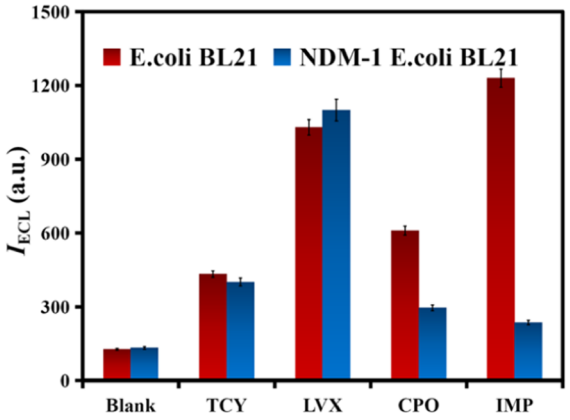


**Figure 4.** ECL intensity of the ECL biosensor incubated with *E. coli* BL21 (red columns) and NDM-1 *E. coli* BL21 (blue columns) treated by the same concentration of antibiotics. Blank represented the sample with no antibiotic incubation.

For normal *E. coli* BL21, as shown in Figure 4 (red columns), the *E. coli* sample without antibiotics showed the lowest ECL intensity (127) since the bacterial cell surface in this sample was intact, which resulted in maximum LPS binding to the Con A-modified ECL biosensor interface. Once the *E. coli*. samples were introduced, the ECL intensity increased to 433, 1030, 610, and 1230 when *E. coli* BL21 was incubated with given concentrations of TCY, LVX, CPO, and IMP, respectively. These results indicated that these antibiotics (TCY, LVX, CPO, and IMP) inhibited the growth of *E. coli* BL21 and the amount of LPS on the bacterial cell wall decreased, which resulted in a smaller number of *E. coli* BL21 binding to the ECL biosensor interface compared to that in the control sample (without antibiotics). Since different kinds of antibiotics have different inhibitory effects on *E. coli* BL21, the binding of *E. coli* on the ECL biosensor surface remains distinctly different. IMP provided stronger antimicrobial susceptibility against *E. coli* BL21 than LVX at the same concentration, and both LVX and CPO were superior to TCY against *E. coli* BL21.

NDM-1, a B1 subclass of metallo-$\beta$-lactamases (M$\beta$Ls),[43] was first found in *Klebsiella pneumoniae* in 2008[44] and spread worldwide rapidly thereafter.[45] NDM-1 hydrolyzes almost all $\beta$-lactam antibiotics, such as penicillins, cephalosporins, and carbapenems.[46] The ECL biosensor reported in this work was also used to evaluate NDM-1 activity in live bacteria. In addition to CPO and IMP as $\beta$-lactam antibiotics, non-$\beta$-lactam variants like TCY and LVX were also selected for the evaluation. As shown in Figure 4 (blue columns), the blank sample without antibiotics provided the lowest ECL intensity (133). The ECL intensity then increased to 401, 1100, 296, and 236 when NDM-1 *E. coli* BL21 was incubated with given concentrations of TCY, LVX, CPO, and IMP, respectively. As evident from Figure 4, the magnitude of the increase in ECL intensity was similar when *E. coli* BL21 and NDM-1 *E. coli* BL21 were incubated with the same concentrations of TCY and LVX, thereby indicating similar bactericidal effects of TCY and LVX on both *E. coli* BL21 and NDM-1 *E. coli* BL21. However, the ECL intensity gained was lower when NDM-1 *E. coli* BL21 was incubated with the same concentrations of CPO and IMP than that when *E. coli* BL21 was incubated under same conditions, highlighting that the bactericidal effects of CPO and IMP against *E. coli* BL21 were stronger than those against NDM-1 *E. coli* BL21. A possible reason for this observation is that CPO and IMP ($\beta$-lactam antibiotics) get hydrolyzed by NDM-1 present in the *E. coli* cell wall[47] and have a weaker inhibitory effect on the growth of NDM-1 *E. coli* BL21. These results are consistent with our initial hypothesis that if antibiotics work on *E. coli*, the binding interaction between *E. coli* LPS and Con A confined to the biosensor surface would be affected, leading to changes in ECL signals. This will be the basis of future work, where the properties of antibiotics and their biological action could be quantified according to these signal changes.

**ECL Biosensors for Antimicrobial Susceptibility against *E. coli* BL21.** To further study the effect of antibiotic concentrations on antimicrobial susceptibility, different concentrations of antibiotics were added into the LB medium containing *E. coli* BL21. Figure 5 depicts ECL intensity as a function of different antibiotic concentrations measured by the ECL biosensor. Further, ECL intensity increased when the same concentration of *E. coli* BL21 was incubated with the increasing concentration of TCY, LVX, CPO, and IMP (Figure 5). As discussed above, higher concentrations of antibiotics have a stronger effect on *E. coli* BL21 that is reflected in the smaller number of *E. coli* BL21 bound to the Con A-modified biosensor. The ECL intensity increased from 127 to 1023 with the increasing concentration of TCY from 0 to 16 mg/L, and the corresponding concentrations of *E. coli* BL21 were $3.7 \times 10^4$ to 396 cells/mL, as calculated using the linear regression equation ($I = -383.8 \log C + 1949.7$) detailed in the Analytical Performance section. MIC is defined as the lowest concentration of an antimicrobial agent that would inhibit the visible growth of a microorganism after overnight incubation.[48] In the present work, MIC values were calculated as the concentration of antibiotics corresponding to 80%

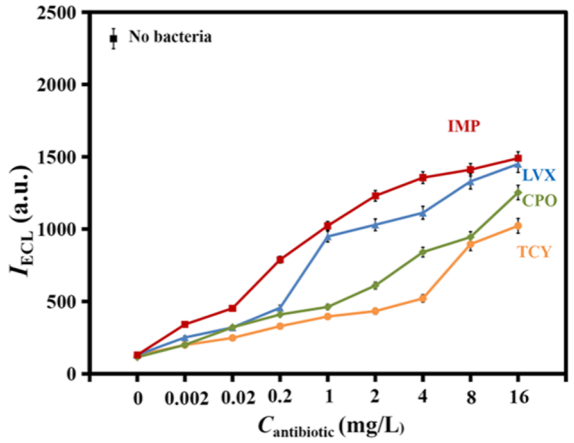


**Figure 5.** Effect of concentrations of antibiotics on the ECL intensity of the ECL biosensor incubated with *E. coli* BL21 treated by the given concentration of antibiotics. The black dot represented the ECL intensity gained from the ECL biosensor without the incubation of bacteria.


https://doi.org/10.1021/acsami.1c11949
ACS Appl. Mater. Interfaces 2021, 13, 38923−38930

reduction in *E. coli* BL21 ($3.7 \times 10^4 \times 0.2 = 7.4 \times 10^3$) compared to the negative control (no antibiotic added to the bacterial suspension). Therefore, the MIC of TCY against *E. coli* BL21 could be deduced to be 2−4 mg/L. Similarly, the MIC values of LVX, CPO, and IMP against *E. coli* BL21 were calculated to be 0.02−0.2, 0.2−1, and 0.002−0.02 mg/L, respectively. The results of Figure 5 showed that IMP has the greatest damage to bacterial LPS, which may be caused by their different mechanisms of action. LVX is the third-generation fluoroquinolone, which initially interacts with bacteria by displacing or binding divalent calcium and magnesium cations in the bacterial outer membrane. LPS may become destabilized and ultimately released from the bacterium when divalent cation bridges are removed from the outer membrane.[49] The $\beta$-lactam antibiotics (CPO and IMP), on the other hand, are not known to interact with divalent cations on the bacterial outer membrane. Instead, these compounds pass through water-filled porin channels and interact with penicillin-binding proteins (PBPs) on the cytoplasmic membrane. Inactivation of PBPs weakens the bacterial cell wall and causes cell lysis.[50] TCY exerts a bacteriostatic effect on bacteria by binding to the bacterial 30S ribosomal subunit and blocking incoming aminoacyl tRNA to the ribosome acceptor site and finally causes intracellular components to leak from bacterial cells.[51] The velocity and amount of LPS released by TCY are largely dependent on its concentration used. Paradoxically, at the highest concentrations of TCY tested, little LPS was released.[51] In our work, the trend of bactericidal activity (i.e., TCY < CPO < LVX < IMP) obtained from the ECL biosensor (shown in Table S1) indicated that the amount of released LPS by IMP is much higher than other antibiotics, given the mechanism of antibiotics and the principle of ECL biosensor-binding bacteria. From Table S1, it can be seen that the MIC trend is somewhat different from the data reported in the literature. The possible reason is that this study based on the relationship between the ECL signal and the antibiotic concentration showed that along with MICs values, there are other parameters that govern this relationship.

**ECL Biosensors for Antimicrobial Susceptibility against NDM-1 *E. coli* BL21.** As discussed, Figure 4 demonstrates that TCY and LVX at a given concentration have similar effects on both *E. coli* BL21 and NDM-1 *E. coli* BL21 strains, whereas NDM-1 *E. coli* BL21 shows resistance to CPO and IMP due to NDM-1 hydrolysis. These results are in overall agreement with the existing literature reporting the hydrolysis of $\beta$-lactam antibiotics by NDM-1 present in the *E. coli* cell wall, while non-$\beta$-lactam antibiotics are not hydrolyzed.[47] Based on these insights, we further investigated the ability of NDM-1 *E. coli* BL21 to hydrolyze different concentrations of CPO and IMP. Figure 6 shows the effect of the increasing concentrations of CPO and IMP on ECL intensity after the ECL biosensor was incubated with antibiotic-treated NDM-1 *E. coli* BL21. ECL intensity increased when NDM-1 *E. coli* BL21 was incubated with increasing concentrations of CPO and IMP. However, the increase in ECL intensity due to the presence of NDM-1 *E. coli* BL21 is clearly lower than that detected by the ECL biosensor incubated with *E. coli* BL21 treated with antibiotics under same concentrations (Figure 5), which implies that the same antibiotics inhibit NDM-1 *E. coli* BL21 to a weaker extent than *E. coli* BL21. This result indicates that $\beta$-lactam antibiotics were hydrolyzed by NDM-1 present in *E. coli* cells. In addition, with increasing antibiotic concentration, the ECL intensity

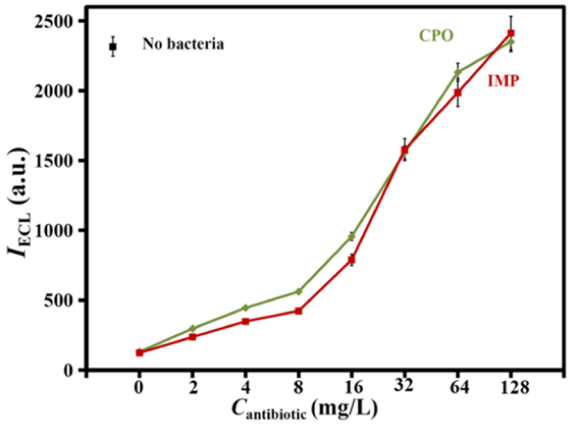


**Figure 6.** Effect of concentrations of antibiotics on the ECL intensity of the ECL biosensor incubated with NDM-1 *E. coli* BL21 treated by the given concentration of antibiotics. The black dot represented the ECL intensity gained from the ECL biosensor without the incubation of bacteria.

increased to the value obtained from the blank signal (black dot in Figure 6, no *E. coli* binding to the ECL biosensor surface). This phenomenon possibly resulted from the fact that higher antibiotic concentrations exert bactericidal effects on the bacteria. Based on the quantitative analysis mentioned above, the MIC value of IMP (~8−16 mg/L) against NDM-1 *E. coli* BL21 was calculated to be higher than that of CPO (~4 mg/L), indicating the greater resistance of NDM-1 *E. coli* BL21 to IMP than that to CPO under the same condition.

## CONCLUSIONS

A novel ECL biosensor, designed to exploit the lectin interaction with LPS on the *E. coli* cell wall, was utilized to detect *E. coli* and evaluate the antimicrobial susceptibility of various antibiotics to normal and drug-resistant *E. coli* strains. The ECL biosensor showed excellent sensitivity (with an appreciably lower detection limit of 11 cells/mL), selectivity, and stability compared to other biosensing methods. The MIC values of TCY, LVX, CPO, and IMP against *E. coli* BL21 were estimated to be 2−4, 0.02−0.2, 0.2−1, and 0.002−0.02 mg/L, respectively. In addition, the MIC value of IMP (~8−16 mg/L) against NDM-1 *E. coli* BL21 was higher than that of CPO (~4 mg/L). Therefore, the ECL biosensor reported here could be advantageous for multiple directions of biosensor development, which attributed to the following advantages: First, the Ru complex attached to the $NH_2$-MIL-53(Al)-modified surface enhance the ECL signal gained, which facilitates the sensitivity of detection. Second, the ECL biosensor designed via Ru complex immobilization solid detection makes the miniaturization of the instrument simple, which avoids the storage of the $Ru(bpy)_3^{2+}$/TPA solution and nonspecific adsorption of $Ru(bpy)_3^{2+}$/TPA on the Con A-modified biosensing surface and bacteria. Third, the covalent attachment of ruthenium complexes to the electrode enhances the stability of the ECL biosensor. Of course, there are also disadvantages, such as Ru-labeled Con A partly affects Con A activity and the coverage of Con A on the $NH_2$-MIL-53(Al)-modified surface. The ECL biosensor could be suitable for rapid, low cost, and sensitive detection of bacterial analytes and ASTs against normal and drug-resistant bacteria, which could lead to novel research directions toward drug discovery for infectious diseases.


https://doi.org/10.1021/acsami.1c11949
ACS Appl. Mater. Interfaces 2021, 13, 38923−38930

## ■ ASSOCIATED CONTENT

### Supporting Information

The Supporting Information is available free of charge at https://pubs.acs.org/doi/10.1021/acsami.1c11949.

Additional information including fabrication of the ECL biosensor; characterization of $NH_2$-MIL-53(Al) nanoplates; and characterization and stability of the ECL biosensor, as noted in the text (PDF)

## ■ AUTHOR INFORMATION


### Corresponding Author

**Fen Ma** − *Key Laboratory of Synthetic and Natural Functional Molecule of the Ministry of Education, College of Chemistry and Materials Science, Northwest University, Xi'an, Shaanxi 710127, People's Republic of China;* orcid.org/0000-0001-6758-2904; Email: mafen@nwu.edu.cn

### Authors

**Lina Sun** − *Key Laboratory of Synthetic and Natural Functional Molecule of the Ministry of Education, College of Chemistry and Materials Science, Northwest University, Xi'an, Shaanxi 710127, People's Republic of China*

**Yu Chen** − *Key Laboratory of Synthetic and Natural Functional Molecule of the Ministry of Education, College of Chemistry and Materials Science, Northwest University, Xi'an, Shaanxi 710127, People's Republic of China*

**Yuhong Duan** − *Key Laboratory of Synthetic and Natural Functional Molecule of the Ministry of Education, College of Chemistry and Materials Science, Northwest University, Xi'an, Shaanxi 710127, People's Republic of China*

Complete contact information is available at: https://pubs.acs.org/10.1021/acsami.1c11949


### Author Contributions

The manuscript was written through contributions of all authors. All authors have given approval to the final version of the manuscript.

### Notes

The authors declare no competing financial interest.

## ■ ACKNOWLEDGMENTS

The authors gratefully acknowledge the financial support from the National Natural Science Foundation of China (21605120). The authors thank Dr. Jiawei Liu for the synthesis of the $NH_2$-MIL-53(Al) nanoplate and Dr. Yuan He for her technical assistance for NDM-1 *E. coli* BL21 in Northwest University.

## ■ REFERENCES


(1) Shen, Z. H.; Huang, M. C.; Xiao, C.; Zhang, Y.; Zeng, X. Q.; Wang, P. G. Nonlabeled Quartz Crystal Microbalance Biosensor for Bacterial Detection Using Carbohydrate and Lectin Recognitions. *Anal. Chem.* **2007**, *79*, 2312−2319.

(2) Shabani, A.; Zourob, M.; Allain, B.; Marquette, C. A.; Lawrence, M. F.; Mandeville, R. Bacteriophage-Modified Microarrays for the Direct Impedimetric Detection of Bacteria. *Anal. Chem.* **2008**, *80*, 9475−9482.

(3) Liang, T.; Leung, L. M.; Opene, B.; Fondrie, W. E.; Lee, Y. I.; Chandler, C. E.; et al. Rapid Microbial Identification and Antibiotic Resistance Detection by Mass Spectrometric Analysis of Membrane Lipids. *Anal. Chem.* **2019**, *91*, 1286−1294.

(4) Yang, K.; Li, H.-Z.; Zhu, X.; Su, J.-Q.; Ren, B.; Zhu, Y.-G.; Cui, L. Rapid Antibiotic Susceptibility Testing of Pathogenic Bacteria Using Heavy-Water-Labeled Single-Cell Raman Spectroscopy in Clinical Samples. *Anal. Chem.* **2019**, *91*, 6296−6303.

(5) Zhu, Y.-G.; Gillings, M.; Simonet, P.; Stekel, D.; Banwart, S.; Penuelas, J. Microbial mass movements. *Science* **2017**, *357*, 1099.

(6) van Belkum, A.; van Bachmann, T. T.; Lüdke, G.; Lisby, J. G.; Kahlmeter, G.; Mohess, A.; Becker, K.; Hays, J. P.; Woodford, N.; Mitsakakis, K.; Moran-Gilad, J.; Vila, J.; Peter, H.; Rex, J. H., Jr.; W, M. D. Developmental roadmap for antimicrobial susceptibility testing systems. *Nat. Rev. Microbiol.* **2019**, *17*, 51−62.

(7) Kang, W.; Sarkar, S.; Lin, Z. S.; McKenney, S.; Konry, T. Ultrafast Parallelized Microfluidic Platform for Antimicrobial Susceptibility Testing of Gram Positive and Negative Bacteria. *Anal. Chem.* **2019**, *91*, 6242−6249.

(8) Opota, O.; Croxatto, A.; Prod'hom, G.; Greub, G. Blood culture-based diagnosis of bacteraemia: state of the art. *Clin. Microbiol. Infect.* **2015**, *21*, 313−322.

(9) Wiegand, I.; Hilpert, K.; Hancock, R. E. W. Agar and broth dilution methods to determine the minimal inhibitory concentration (MIC) of antimicrobial substances. *Nat. Protoc.* **2008**, *3*, 163−175.

(10) Tang, Y. Y.; Zhen, L.; Liu, J. Q.; Wu, J. M. Rapid Antibiotic Susceptibility Testing in a Microfluidic pH Sensor. *Anal. Chem.* **2013**, *85*, 2787−2794.

(11) Murray, C.; Adeyiga, O.; Owsley, K.; Carlo, D. D. Research highlights: microfluidic analysis of antimicrobial susceptibility. *Lab Chip* **2015**, *15*, 1226−1229.

(12) Schoepp, N. G.; Khorosheva, E. M.; Schlappi, T. S.; Curtis, M. S.; Humphries, R. M.; Hindler, J. A.; Ismagilov, R. F. Digital Quantification of DNA Replication and Chromosome Segregation Enables Determination of Antimicrobial Susceptibility after only 15Minutes of Antibiotic Exposure. *Angew. Chem., Int. Ed.* **2016**, *55*, 9557−9761.

(13) Mezger, A.; Gullberg, E.; Göransson, J.; Zorzet, A.; Herthnek, D.; Tano, E.; Nilsson, M.; Andersson, D. I. A General Method for Rapid Determination of Antibiotic Susceptibility and Species in Bacterial Infections. *J. Clin. Microbiol.* **2015**, *53*, 425.

(14) Schoepp, N. G.; Schlappi, T. S.; Curtis, M. S.; Butkovich, S. S.; Miller, S.; Humphries, R. M.; Ismagilov, R. F. Rapid pathogen-specific phenotypic antibiotic susceptibility testing using digital LAMP quantification in clinical samples. *Sci. Transl. Med.* **2017**, *9*, No. eaal3693.

(15) Reller, L. B.; Weinstein, M.; Jorgensen, J. H.; Ferraro, M. J. Antimicrobial Susceptibility Testing: A Review of General Principles and Contemporary Practices. *Clin. Infect. Dis.* **2009**, *49*, 1749−1755.

(16) Notomi, T.; Mori, Y.; Tomita, N.; Kanda, H. Loop-mediated isothermal amplification (LAMP): principle, features, and future prospects. *J. Microbiol.* **2015**, *53*, 1−5.

(17) Chang, K.-W.; Cheng, H.-W.; Shiue, J.; Wang, J.-K.; Wang, Y.-L.; Huang, N.-T. Antibiotic Susceptibility Test with Surface-Enhanced Raman Scattering in a Microfluidic System. *Anal. Chem.* **2019**, *91*, 10988−10995.

(18) Klein, D. R.; Powers, M. J.; Trent, M. S.; Brodbelt, J. S. Top-Down Characterization of Lipooligosaccharides from Antibiotic-Resistant Bacteria. *Anal. Chem.* **2019**, *91*, 9608−9615.

(19) Mo, M.; Yang, Y.; Zhang, F.; Jing, W.; Iriya, R.; Popovich, J.; Wang, S. P.; Grys, T.; Haydel, S. E.; Tao, N. J. Rapid Antimicrobial Susceptibility Testing of Patient Urine Samples Using Large Volume Free-Solution Light Scattering Microscopy. *Anal. Chem.* **2019**, *91*, 10164−10171.

(20) Croxatto, A.; Prod'hom, G.; Greub, G. Applications of MALDI-TOF mass spectrometry in clinical diagnostic microbiology. *Fems Microbiol. Rev.* **2012**, *36*, 380−407.

(21) Andersson, M.; Carlin, N.; Leontein, K.; Lindquist, U.; Slettengren, K. Structural studies of the O-antigenic polysaccharide of Escherichia coli O86, which possesses blood-group B activity. *Carbohydr. Res.* **1989**, *185*, 211−223.

(22) Hsu, K.-L.; Pilobello, K. T.; Mahal, L. K. Analyzing the dynamic bacterial glycome with a lectin microarray approach. *Nat. Chem. Biol.* **2006**, *2*, 153−157.

(23) Ma, F.; Rehman, A.; Liu, H. Y.; Zhang, J. T.; Zhu, S. L.; Zeng, X. Q. Glycosylation of quinone-fused polythiophene for reagentless and label-free detection of E. coli. *Anal. Chem.* **2015**, *87*, 1560−1568.
(24) Zhou, J.; Butchosa, N.; Jayawardena, H. S.; Zhou, Q.; Yan, M.; Ramstrom, O. Glycan-functionalized fluorescent chitin nanocrystals for biorecognition applications. *Bioconjugate Chem.* **2014**, *25*, 640−643.
(25) Chen, X. J.; Wang, Y. Z.; Zhang, Y. Y.; Chen, Z. H.; Liu, Y.; Li, Z. L.; Li, J. H. Sensitive Electrochemical Aptamer Biosensor for Dynamic Cell Surface N-Glycan Evaluation Featuring Multivalent Recognition and Signal Amplification on a Dendrimer−Graphene Electrode Interface. *Anal. Chem.* **2014**, *86*, 4278−4286.
(26) Wurpel, D. J.; Totsika, M.; Allsopp, L. P.; Hartley-Tassell, L. E.; Day, C. J.; Peters, K. M.; Sarkar, S.; Ulett, G. C.; Yang, J.; Tiralongo, J.; Strugnell, R. A.; Jennings, M. P.; Schembri, M. A. F9 Fimbriae of Uropathogenic Escherichia coli Are Expressed at Low Temperature and Recognise Gal$\beta$1-3GlcNAc-Containing Glycans. *PLoS One* **2014**, *9*, No. e93177.
(27) Van Den Berg, C.; de Neeling, A. J.; Schot, C. S.; Hustinx, W. N.; Wemer, J.; de Wildt, D. J. Delayed antibiotic-induced lysis of Escherichia coli in vitro is correlated with enhancement of LPS release. *Scand. J. Infect. Dis.* **1992**, *24*, 619−627.
(28) Ma, F.; Rehman, A.; Sims, M.; Zeng, X. Q. Antimicrobial susceptibility assays based on the quantification of bacterial lipopolysaccharides via a label free lectin biosensor. *Anal. Chem.* **2015**, *87*, 4385−4393.
(29) Richter, M. M. Electrochemiluminescence (ECL). *Chem. Rev.* **2004**, *104*, 3003−3036.
(30) Qi, H. L.; Zhang, C. X. Electrogenerated Chemiluminescence Biosensing. *Anal. Chem.* **2020**, *92*, 524−534.
(31) Lin, X. M.; Luo, F. Q.; Zheng, L. Y.; Gao, G. M.; Chi, Y. W. Fast, Sensitive, and Selective Ion-Triggered Disassembly and Release Based on Tris(bipyridine)ruthenium(II)-Functionalized Metal−Organic Frameworks. *Anal. Chem.* **2015**, *87*, 4864−4870.
(32) Zhang, S. P.; Zheng, H. L.; Chen, Y. J.; Li, H.; Dai, H.; Hong, Z. S.; Lin, Y. Y. Electrochemluminescence Resonance Energy Transfer between $Ru(bpy)_3^{2+}$ and CdZnSe@Znse Quantum Dots for Ovarian Cancer Biomarker Detection. *ACS Appl. Nano Mater.* **2019**, *2*, 7061−7066.
(33) Wang, B.; Jing, R.; Qi, H. L.; Gao, Q.; Zhang, C. X. Label-free electrochemical impedance peptide-based biosensor for the detection of cardiac troponin I incorporating gold nanoparticles modified carbon electrode. *J. Electroanal. Chem.* **2016**, *781*, 212−217.
(34) Jeong, H.; Barbe, V.; Lee, C. H.; Vallenet, D.; Yu, D. S.; Choi, S.-H.; Couloux, A.; Lee, S.-W.; Yoon, S. H.; Cattolico, L.; Hur, C.-G.; Park, H.-S.; Ségurens, B.; Kim, S. C.; Oh, T. K.; Lenski, R. E.; Studier, F. W.; Daegelen, P.; Kim, J. F. Genome Sequences of Escherichia coli B strains REL606 and BL21(DE3). *J. Mol. Biol.* **2009**, *394*, 644−652.
(35) Marolda, C. L.; Feldman, M. F.; Valvano, M. A. Genetic organization of the O7-specific lipopolysaccharide biosynthesis cluster of Escherichia coli VW187 (O7:K1). *Microbiology* **1999**, *145*, 2485−2495.
(36) Pistole, T. G. Interaction of Bacteria and Fungi with Lectins and Lectin-Like Substances. *Annu. Rev. Microbiol.* **1981**, *35*, 85−112.
(37) Kaiser, H. Guiding Concepts Relating to Trace Analysis. *J. Pure Appl. Chem.* **1973**, *34*, 35−62.
(38) Sun, J.; Warden, A. R.; Huang, J.; Wang, W.; Ding, X. Colorimetric and Electrochemical Detection of Escherichia coli and Antibiotic Resistance Based on a p-Benzoquinone-Mediated Bioassay. *Anal. Chem.* **2019**, *91*, 7524−7530.
(39) Sun, X.; Wang, Y.; Zhang, L.; Liu, S.; Zhang, M.; Wang, J.; Ning, B. A.; Peng, Y.; He, J.; Hu, Y. G.; Gao, Z. X. CRISPR-Cas9 Triggered Two-Step Isothermal Amplification Method for E. coli O157:H7 Detection Based on a Metal-Organic Framework Platform. *Anal. Chem.* **2020**, *92*, 3032−3041.
(40) Lis, H.; Sharon, N. Lectins as Molecules and as Tools. *Annu. Rev. Biochem.* **1986**, *55*, 35−67.
(41) Evans, M. E.; Pollack, M. Effect of Antibiotic Class and Concentration on the Release of Lipopolysaccharide from Escherichia coli. *J. Infect. Dis.* **1993**, *167*, 1336−1343.
(42) Leive, L. The barrier function of the gram-negative envelope. *Ann. N. Y. Acad. Sci.* **1974**, *235*, 109−129.
(43) Bush, K.; Jacoby, G. A. Updated Functional Classification of $\beta$-Lactamases. *Antimicrob. Agents Chemother.* **2010**, *54*, 969.
(44) Yong, D.; Toleman, M. A.; Giske, C. G.; Cho, H. S.; Sundman, K.; Lee, K.; Walsh, T. R. Characterization of a New Metallo-$\beta$-Lactamase Gene, bla(NDM-1), and a Novel Erythromycin Esterase Gene Carried on a Unique Genetic Structure in Klebsiella pneumoniae Sequence Type 14 from India. *Antimicrob. Agents Chemother.* **2009**, *53*, 5046.
(45) Walsh, T. R. Emerging carbapenemases: a global perspective. *Int. J. Antimicrob. Agents* **2010**, *36*, S8−S14.
(46) Cornaglia, G.; Giamarellou, H.; Rossolini, G. M. Metallo-$\beta$-lactamases: a last frontier for $\beta$-lactams? *Lancet Infect. Dis.* **2011**, *11*, 381−393.
(47) Yang, K. W.; Zhou, Y.; Ge, Y.; Zhang, Y. J. Real-time activity monitoring of New Delhi metallo-beta-lactamase-1 in living bacterial cells by UV-Vis spectroscopy. *Chem. Commun.* **2017**, *53*, 8014−8017.
(48) Andrews, J. M. Determination of minimum inhibitory concentrations. *J. Antimicrob. Chemother.* **2001**, *48*, 5−16.
(49) Chapman, J. S.; Georgopapadakou, N. H. Routes of quinolone permeation in Escherichia coli. *Antimicrob. Agents Chemother.* **1988**, *32*, 438−442.
(50) Hancock, R. E. W.; Bell, A. Antibiotic uptake into gram-negative bacteria. *Eur. J. Clin. Microbiol. Infect. Dis.* **1988**, *7*, 713−720.
(51) Evans, M. E.; Pollack, M. Effect of Antibiotic Class and Concentration on the Release of Lipopolysaccharide from Escherichia coli. *J. Infect. Dis.* **1993**, *167*, 1336−1343.


https://doi.org/10.1021/acsami.1c11949
*ACS Appl. Mater. Interfaces* 2021, 13, 38923−38930